Bromodomain Inhibition Blocks Inflammation-Induced Cardiac Dysfunction and SARS-CoV2 Infection in Pre-Clinical Models

Richard J Mills[1], Sean J Humphrey[2], Patrick RJ Fortuna[1], Gregory A Quaife-Ryan[1], Mary Lor[1], Rajeev Ruraraju[3,4,5], Daniel J Rawle[1], Thuy Le[1] Wei Zhao[5], Leo Lee[5], Charley Mackenzie-Kludas[5], Neda R Mehdiabadi[6], Lynn Devilée[1], Holly K Voges[1], Liam T Reynolds[1], Sophie Krumeich[1], Ellen Mathieson[1], Dad Abu-Bonsrah[6,7], Kathy Karavendzas[6], Brendan Griffen[8], Drew Titmarsh[8], David A Elliott[6], James McMahon[9,10], Andreas Suhrbier[1,11], Kanta Subbarao[3,5], Enzo R Porrello[6,12], Mark J Smyth[1], Christian R Engwerda[1], Kelli PA MacDonald[1], Tobias Bald[1], David E James[2,13], James E Hudson[1,*]

[1]QIMR Berghofer Medical Research Institute, Brisbane 4006, QLD, Australia
[2] Charles Perkins Centre, School of Life and Environmental Science, The University of Sydney, Sydney 2006, NSW, Australia
[3]The WHO Collaborating Centre for Reference and Research on Influenza, The Peter Doherty Institute for Infection and Immunity, Melbourne 3052, VIC, Australia
[4]Department of Microbiology and Immunology, The University of Melbourne, Melbourne 3052, VIC, Australia
[5]The Peter Doherty Institute for Infection and Immunity, Melbourne 3052, VIC, Australia
[6]Murdoch Children's Research Institute, The Royal Children's Hospital, Melbourne 3052, VIC, Australia
[7]Department of Paediatrics, The University of Melbourne, Melbourne 3052, VIC, Australia
[8]Dynomics Inc., San Mateo, CA 94401, United States of America and Dynomics Pty Ltd, Brisbane, QLD 4000, Australia
[9]Department of Infectious Diseases, The Alfred Hospital and Monash University, Melbourne VIC 3004, Australia
[10]Department of Infectious Diseases, Monash Medical Centre, Clayton VIC 3168, Australia
[11]GVN Center of Excellence, Australian Infectious Diseases Research Centre, Brisbane, Qld. 4006 and 4072, Australia
[12]Department of Physiology, School of Biomedical Sciences, The University of Melbourne, Melbourne 3052, VIC, Australia
[13]Faculty of Medicine and Health, The University of Sydney, Sydney, NSW 2006, Australia
* Corresponding author

Please address correspondence to:
Associate Professor James E. Hudson
QIMR Berghofer Medical Research Institute
Herston, Brisbane
QLD, 4006, Australia
Tel: +61 7 3362 0141
Email: james.hudson@qimrberghofer.edu.au

ABSTRACT

Cardiac injury and dysfunction occur in COVID-19 patients and increase the risk of mortality. Causes are ill defined, but could be through direct cardiac infection and/or 'cytokine-storm' induced dysfunction. To identify mechanisms and discover cardio-protective therapeutics, we use a state-of-the-art pipeline combining human cardiac organoids with high throughput phosphoproteomics and single nuclei RNA sequencing. We identify that 'cytokine-storm' induced diastolic dysfunction can be caused by a cocktail of interferon gamma, interleukin 1β and poly(I:C) and also human serum from COVID-19 patients. Bromodomain protein 4 (BRD4) is activated along with pathology driving fibrotic and induced nitric oxide synthase genes. BRD inhibitors fully recover function in hCO and completely prevent death in a cytokine-storm mouse model. BRD inhibition decreases transcription of multiple genes, including fibrotic, induced nitric oxide synthase and ACE2, and reduces cardiac infection from SARS-CoV2. Thus, BRD inhibitors are promising candidates to prevent COVID-19 mediated cardiac damage.

MAIN

SARS-CoV2 infection leads to cardiac injury and dysfunction in 20-30% of hospitalized patients (*1*) and higher rates of mortality in patients with pre-existing cardiovascular disease (*2, 3*). Inflammatory factors released as part of the 'cytokine storm' are thought to play a critical role in cardiac dysfunction in severe COVID-19 patients (*4*). The cardiac sequelae reported in patients with COVID-19, include acute coronary syndromes, cardiomyopathy, acute pulmonary heart disease, arrhythmias and heart failure (*5*). There have been multiple proposed aetiologies for these, yet clear mechanistic insight is lacking (*5*). There is a severe inflammatory response in 5% of COVID-19 patients, associated with septic shock (*2*). This leads to a drop in blood pressure, and approximately 30% of hospitalized patients with COVID-19 require vasopressors to improve blood pressure (*6*). Furthermore, 68-78% have sustained cardiac dysfunction, primarily right ventricle dysfunction and left ventricular diastolic dysfunction (*7, 8*).

In severe infections, inflammation associated with a 'cytokine storm' can cause cardiac dysfunction and pathology. COVID-19 induces a cytokine storm of similar magnitude to that induced by CAR-T cell-associated cytokine storms (*9*). Additionally, the severe COVID-19 is associated with sepsis and bacterial products in the serum (*10*), which are known drivers of cardiac pathology and dysfunction. In the absence of infection, well known inflammatory mediators such as TNF are associated with heart failure and have been demonstrated to induce systolic dysfunction (*11*). Thus, inflammation could be a major primary mediator of cardiac injury and dysfunction in COVID-19 patients, and would have further pathological consequences including inadequate organ perfusion and immune cell infiltration, further exacerbating disease. Thus, preventing cytokine-induced cardiac dysfunction may limit severe outcomes in COVID-19 patients. However, targeted treatment strategies, particularly in severe infections such as COVID-19, are currently lacking.

Several anti-inflammatory agents have shown clinical benefit for the acute management of COVID-19. Dexamethasone improved 28-day mortality in COVID-19 patients receiving invasive mechanical ventilation or oxygen at randomization (*12*). Additionally, Janus kinase (JAK)/signal transducer and activator of transcription (STAT) (ruxolitinib and baricitinib) and IL-6R inhibitors (tocilizumab and sarilumab) are currently in COVID-19 clinical trials. However, systemic immunosuppression may impede viral clearance thus potentially exacerbating disease (*13*). To circumvent this, we aimed to identify cardiac-specific inflammatory targets that trigger cardiac dysfunction in response to the cytokine storm, reasoning that these might provide a safe and effective therapeutic option.

Here, we utilize multi-cellular human pluripotent stem cell-derived cardiac organoids (hCO) combined with phosphoproteomics and single nuclei RNA-sequencing to identify therapeutic targets and treatments for cardiac dysfunction. We recently adapted our hCO system (*14, 15*) to include co-culture with endothelial cells that form enhanced branched endothelial structures surrounded by pericytes (**Fig. S1**), together with an optimized culture environment that reflects a maturation stage; mimicking the postnatal metabolic environment (*15*) followed by reversion to a more adult metabolic substrate provision (see **Methods**). This platform enabled rapid screening of cytokine combinations that mimic the COVID-19-induced 'cytokine storm' and cardiac dysfunction, with subsequent application of omic assays and drug screening (*13*).

Cytokine-induced cardiac dysfunction

We began by examining the effects of a range of pro-inflammatory cytokines on cardiac function in our hCO (*13, 16*). Inflammatory molecules tested were TNF, IL-1β, IFN-γ, IL-6, IL-17A, and G-CSF, as well as pathogen-associated molecular patterns including poly(I:C) to mimic dsRNA, and lipopolysaccharide (LPS) to mimic TLR4 activation and septic responses.

Using RNA-seq (*15, 17*), we identified that the expression of the receptors *IL1R1, TNFRSF1A, TNFRSF1B, IFIH1, MYH88, IL6ST, IFNAR1, IL6R, TMEM173, IL17RA, IL17RB, IL17RC, IL17RD, IL17RE, IFNGR1, TLR3*, and *TLR4* were at similar or higher levels in our hCO compared to adult human heart (**Fig. S2A**). In adult mouse hearts many of these are enriched in non-myocyte populations (*18*) (**Fig. S2B**). We used single nuclei RNA sequencing (snRNA-seq) to assess cell specificity in our enhanced hCO (Voges et al., In Revision). Mapping to human heart snRNA-seq (*19*) revealed the presence of pro-epicardial/epicardial cells, fibroblasts, activated fibroblasts/pericytes and cardiomyocytes (**Fig. S2C,D**). Some cardiomyocytes were fetal-like, however there was a distinct sub-cluster that mapped adjacent to adult ventricular cardiomyocytes from human hearts (*20*) (**Fig. S2E**). The cytokine/pro-inflammatory receptors were expressed across different cell types, but were enriched and more highly expressed in epicardial cells and fibroblasts (**Fig. S2F**) (*15, 17*). We screened inflammatory factors in all pair-wise combinations in hCOs with multiple functional measurements including contractile force, rate, activation kinetics and relaxation kinetics (*14, 15*) (**Fig. 1A**). TNF caused a reduction in force, while IFN-γ, IL-1β, poly(I:C) and LPS caused diastolic dysfunction characterized by a preserved contractile force but prolonged time from peak to 50% relaxation (**Fig. S3**). A secondary full-factorial screen of TNF, IFN-γ, IL-1β, and poly(I:C), once again revealed that TNF induced systolic dysfunction (**Fig. 1B,D**) with an EC_{50} of 1 ng/mL at 48 hours (**Fig. S4A**). A combination of IFN-γ, IL-1β and poly(I:C) induced diastolic dysfunction (**Fig. 1c,e**), however also decreased the beating rate which may influence the kinetics of contraction (**Fig. S5, Supplementary Video 1,2**). Changes in rate were not responsible for increased relaxation time, as hCO paced at 1 Hz retained the severe diastolic dysfunction phenotype (**Fig. 1F, Supplementary Video 3,4**). Individually, IFN-γ and IL-1β caused concentration-dependent diastolic dysfunction with a low EC_{50} of 0.8 ng/mL at 48 hours and 3 ng/mL at 24 hours, respectively, while poly(I:C) was not able to induce dysfunction alone (**Fig. S4B to D**). These results were confirmed in an independent cell line and overall the combination of IFN-γ, IL-1β and poly(I:C) induced the most consistent, robust diastolic dysfunction (**Fig. S6A to E**). Taken together this demonstrates that TNF induces systolic dysfunction consistent with previous *in vitro (21)* and *in vivo (22)* studies and the combination of IFN-γ, IL-1β and poly(I:C) induces severe diastolic dysfunction in hCO. The dominant factor identified causing diastolic dysfunction, IFN-γ (**Fig. S6C**), is generally elevated in heart failure patients, but its role in heart failure is contradictory in animal models with both detrimental and beneficial effects reported (*23*).

Mechanisms driving cardiac cytokine storm-induced dysfunction

The most common cardiac dysfunction in hospitalized COVID-19 patients is right ventricular dysfunction or left ventricular diastolic dysfunction (*7*). Therefore, we chose to interrogate the mechanism of diastolic dysfunction induced by IFN-γ, IL-1β and poly(I:C), from here on referred to as 'cardiac cytokine storm' (CS). Since protein phosphorylation is intimately linked with all biological functions (*24*) we reasoned that measuring the global phosphoproteome in hCO would provide an accurate fingerprint of the mechanistic targets of the CS. Employing the latest developments of our phosphoproteomics technology (*25, 26*), enabled identification of over 7,000 phosphosites in each sample, accurately pinpointing 7,927 phosphorylation sites to a single amino acid residue on around 3,000 different phosphoproteins from single-run measurements of 20 organoids yielding < 100 μg of protein each (**Fig. 2A**, **Fig. S7**). Preliminary studies using TNF identified several known biological effects of this cytokine including decreased phosphorylation of protein kinase A and increased phosphorylation of ADRK1 (also known as GRK2), supporting our approach. Applying this technology to the CS treatment revealed 91 phosphosites that were consistently elevated across three biological replicates (**Fig. 2B**). These sites were enriched

for terms relating to proliferation, with transcription factors over-represented with 35 sites found on transcription factors or chromatin-binding proteins and 13 associated with the biological process term 'cell proliferation' (FDR < 0.05, Fisher's exact test). Among these was phosphorylation of signal transducer and activator of transcription 1 (STAT1) S727 (median 13.9 fold), as well as two sites on BRD4 (Bromodomain-containing protein 4) S469 and S1083 (median 7.4 and 12.3 fold respectively) (**Fig 2B,C**). In view of the availability of specific small molecule inhibitors for each of these targets or their upstream regulators we focused on these proteins in subsequent functional assays. The cytokine receptor enrichment in non-myocytes (**Fig. S2**) and broad expression of key phosphorylation sites such as BRD4 (**Fig. 2B**) suggests a multi-cellular response mediates cardiac dysfunction. We assessed activation of individual cell populations in hCOs using snRNA-seq of ~40 pooled hCOs per condition (**Fig. 3A**) with mapping as described above (CTRL - **Fig. S2C,D** and CS - **Fig. S8A,B**). In CS conditions there was an increase in fibroblast and activated fibroblast number (**Fig. 3B**). Consistently, recently identified markers of fibroblast activation (*27*) also increased, including *MEOX1*, *SERPINE1* (also known as plasminogen activator inhibitor-1 which induces clotting), *TNC*, *VEGFC*, and *IL4R*, (**Fig. 3C,D**). Fibroblast activation is known to be widely associated with cardiac dysfunction, including in patients with diastolic dysfunction (*28*).

Drugs for the prevention of cardiac dysfunction

We next screened drugs that could potentially prevent cardiac dysfunction under either TNF-induced systolic dysfunction or CS-driven diastolic dysfunction (**Fig. 4A**). TNF is known to induce systolic dysfunction via GRK2 mediated repression of β-adrenergic receptor signaling (*21*). The selective serotonin reuptake inhibitor, paroxetine hydrochloride, can inhibit GRK2 (*29*), but we found that it was toxic at effective *in vitro* concentrations (*30*) (**Fig. S9A**). GRK2 mediates receptor endocytosis (*31*), and baricitinib was recently identified as a potential AAK1-mediated endocytosis inhibitor using machine learning (*32*). Baricitinib prevented TNF-induced dysfunction in hCO (**Fig. 4B** and **Fig. S9A,B**). However, baricitinib was only protective against TNF-induced systolic dysfunction when co-administered with TNF and was not effective after 24 h TNF treatment (**Fig. 4C**), potentially because receptor internalization had already occurred. Additionally, hCO did not recover quickly from TNF-induced systolic dysfunction after the removal of TNF (**Fig. 4C**) indicating that secondary remodeling events may have occurred.

A key signature of diastolic dysfunction under CS conditions was elevated phosphorylation of transcriptional regulators. STAT1-S727 (**Fig. 2C**) is associated with assembly into chromatin and is required for STAT1 transcriptional and biological activity in response to IFN-γ (*33*). The putative STAT1-S727 kinase is CDK8 (*34*), so we next tested two CDK8 inhibitors SEL120-34A (*35*) and BI-1347 (*36*) previously shown to reduce STAT1-S727 phosphorylation. We also tested baricitinib and ruxolitinib two inhibitors of the JAK/STAT pathway. However, none of these compounds, nor a broader spectrum CDK inhibitor flavopiridol, prevented the CS-induced diastolic dysfunction (**Fig. S10**), noting that flavipiridol was toxic and reduced force and hence all kinetic parameters. Notably, SEL120-34A and BI-1347 specifically attenuated the rate and activation time defects under CS conditions (**Fig. S10B,C,E,F**), which we validated in additional experiments (**Fig. S11A to D**) and may still have clinical utility in this setting.

We observed elevated phosphorylation of the epigenetic regulator BRD4 in our CS treated hCO phosphoproteome. We have previously shown that BRD inhibitors reduce relaxation time in immature hCO (*14*), so we next evaluated the BRD inhibitors INCB054329 (*37*), JQ-1 (*38*), and ABBV-744 (*39*). Strikingly, INCB054329 prevented CS-induced diastolic dysfunction in a dose-dependent manner (**Fig. 4D, Fig. S12**) without affecting force or rate (**Fig. S10A to G, Supplementary Video 5**). JQ-1 also showed improved diastolic function in one hPSC line at the highest concentration (**Fig. S10H**), so an additional higher

concentration for both JQ-1 and ABBV-744 were tested. JQ-1 protected hCO against CS-induced diastolic dysfunction, although INCB054329 was the most efficacious (**Fig. S13A,B**). ABBV-744 was not effective, possibly because it is also an androgen receptor inhibitor, which causes diastolic dysfunction in human cardiomyocytes (*40*). INCB054329 restored diastolic function following 24 h of CS conditions (**Fig. 4E**). This is potentially because CS-induced diastolic dysfunction is driven by the presence of the inflammatory mediators, demonstrated by partial hCO recovery 24 h after removing CS factors (**Fig. 4E**). In patients, all inflammatory factors may be present simultaneously, and we found that INCB054329 could attenuate diastolic dysfunction with all four factors, TNF, IFN-γ, IL-1β, and poly(I:C), present (**Fig. S13C**).

Diastolic dysfunction in hCO and human patients with heart failure with preserved ejection fraction (HFpEF) or COVID-19 is associated with fibrosis (*28, 41*) (**Fig. 3**), with BRD4 known to activate extracellular matrix deposition by fibroblasts (*42, 43*). In addition to this potential mechanism, chronic inflammation caused by obesity, diabetes mellitus, chronic obstructive pulmonary disease, and hypertension cause systemic inflammation which also drives endothelial dysfunction and decreased nitric oxide (NO) availability (*44*). This causes iNOS compensation in other cell types, which can cause nitrosylation stress and cardiac dysfunction (*45, 46*). As BRD4 is broadly expressed in our hCO (**Fig. 4F**), BRD4 inhibition may also protect against these changes. We found CS decreased *NOS3* mRNA (also known as *eNOS*) and induced *NOS2* mRNA (also known as *iNOS*) ~40 fold in hCO, which in turn could be fully prevented by BRD inhibition without rescue of *eNOS* (**Fig. 4G**).

We next assessed whether human serum from COVID-19 patients could induce dysfunction in hCO (**Fig. 4H**). Interestingly, levels of acute cardiac damage (cardiac troponin I, CTNI) and cardiac stress (brain natriuretic peptide, BNP) were elevated in 'mild' rather than severe patients in our cohort (**Fig. 4H**). Using our platform we were able to demonstrate that hCO function was dictated by factors present in the human serum, as patients receiving noradrenaline as inotropic support elevated contractile force in our hCO (**Fig. 4H**). Human COVID-19 patient serum with elevated CTNI and BNP caused diastolic dysfunction in hCO (**Fig. 4H**). INCB054329 prevented diastolic dysfunction caused by serum with the highest levels of CNTI and BNP, and had no effect on function in hCO treated with serum with the lowest levels of CNTI and BNP (which did not induce dysfunction and was free from inotropes) (**Fig. 4I**).

INCB054329 prevents death in a cytokine storm model

There are currently no reported animal models that recapitulate the cytokine storm following SARS-CoV2 infection that has been observed in humans. We therefore tested the ability of INCB054329 to prevent LPS-induced cytokine storm and lethality *in vivo* (**Fig. 5A**). LPS induced pro-inflammatory cytokines TNF, IL-1β and IFN-γ, which were elevated in the plasma (**Fig. 5B**) and induced in the heart (**Fig. 5C**). Treatment with INCB054329 blocked the LPS-induced pro-inflammatory cytokine production (**Fig. 5B,C**). LPS induced a fibrotic response in the heart including induction of *Meox1* and *Tnc* but not *Postn*, consistent with our data in hCO (**Fig. 3**), which was also blocked by INCB054329 (**Fig. S14**). Also, consistent with data in hCO, LPS reduced *eNos* and induced *iNos* which was blocked by INCB054329 without rescue of *eNos* (**Fig. 5D**). *Nppb* was also reduced, consistent with a reduction in LPS-induced cardiac stress (**Fig. 5E**). We observed a marked improvement in mortality, whereby all INCB054329-treated mice survived after 24 h of the LPS-challenge, compared with only 25% in the control group (**Fig. 5F**). INCB054329 therefore has potent and robust effects on improving of cardiac pathological markers and cytokine storm-induced mortality.

INCB054329 protects against SARS-CoV2 infection

SARS-CoV2 can infect human pluripotent stem cell-derived cardiomyocytes (hPSC-CM) (*47*). We tested whether BRD inhibition would potentially exacerbate infection/death (**Fig. 6A**). We confirmed these findings and show that infection of 2D cultured hPSC-CM increases over time (**Fig. S15A**), dsRNA is present in infected hPSC-CM (**Fig. S15B**) and there is live viral replication in infected hPSC-CM (**Fig. S15C**). Increasing viral titres increased cell death (**Fig. S15D**) and even low titres resulted in intracellular viral infection and death over 7 days (**Fig. S15D,E**). Low titres of 0.01 MOI could infect mature hCO, demonstrating that this was not due to hPSC-CM immaturity (**Fig. S15F**). However, hCO infection was ~100 fold lower than 2D culture and there were no gross effects on sarcomere organisation in the hCO (**Fig. S15F,G**), indicating localized infection. We therefore chose to assess the effects of BRD inhibition on viral replication in 2D hPSC-CM (**Fig. 6A**). Treatment with INCB054329 at the time of infection did not change viral load or replication (**Fig. S15H,I,J**). As patients may receive BRD inhibitors prior to infection of the heart, we also assessed the impact of a treatment combined with 3 day pre-incubation of INCB054329. This resulted in a >4 fold decrease in viral load (**Fig. 6B**), potentially via decreased ACE2 expression (**Fig. 6C**). Treatment with INCB054329 also prevented cardiomyocyte sarcomere loss caused by infection (**Fig. 6D,E**) and drastically reduced the presence of infected cells **Fig. S15K**). This indicates that pre-treatment with BRD inhibitors confers some protection of the heart to SARS-CoV2 infection, making them very promising therapeutics for the prevention of cardiac injury and dysfunction for patients with COVID-19.

DISCUSSION

Cardiac dysfunction may be caused by systemic cytokine storm (*9*) or locally induced cardiac viral toxicity or cytokine production (*48*). In this study we show that inflammatory mediators directly impact cardiac function in hCO, a model free from the secondary effects and neurohormonal compensation present *in vivo*. We find that a combination of classical viral response cytokines IFN-γ and IL-1β, combined with dsRNA – 'CS' - cause severe diastolic dysfunction with 20-50% increases in relaxation time without decline in systolic function. This is consistent with clinical data from HFpEF patients, where cardiomyocytes have increased time to 50% relaxation by ~13-18% (with similar overall values of 100-150 ms in both humans and hCO) (*49*). A reason why cardiovascular risk factors for HFpEF are also risk factors for mortality in COVID-19 patients, may be that the underlying chronic inflammation and cardiac dysfunction becomes further exacerbated by the acute, inflammatory response in patients with COVID-19. Prolonged relaxation also increases the risk of arrhythmias, which have been widely reported in COVID-19 patients (*50*). Arrhythmic events increased in CS conditions across our 7 experiments, for which INCB054329 also conferred protection (**Fig. S16A to C**).

By performing high-sensitivity phsophoproteomics and drug screening with our optimized hCO platform we identify a therapeutically targetable inflammation-BRD4 -fibrosis/iNOS axis. This acts as a key intracellular mediator of inflammation-induced cardiac dysfunction, which functions independently of JAK/STAT. BRD4 inhibition reduced inflammatory cytokine production, fibroblast activation, and compensatory iNOS production, all of which drive cardiac dysfunction.

Previously, the BRD inhibitor GSK525762A has shown efficacy in mouse cytokine storm models (*51*) and JQ-1 has shown efficacy in small animal cardiac injury models (*52*). However, in our studies INCB054329 was far more potent than JQ-1, and ABBV-744 had no efficacy in improving CS induced dysfunction. This indicates that BRD inhibitors need to be carefully selected for cardiac efficacy, despite their broad utility for a variety of clinical conditions (*53*).

We demonstrate that BRD inhibitors are powerful drugs to attenuate cardiac dysfunction and prevent cardiac infection. Additionally, we also show anti-inflammatory and anti-fibrotic effects, which may have benefits in multiple organs affected by COVID-19 including the lungs (*43*). Taken together, the efficacy and known safety profile of BRD inhibitors make them prime candidates for drug repurposing for COVID-19 to improve morbidity and mortality.
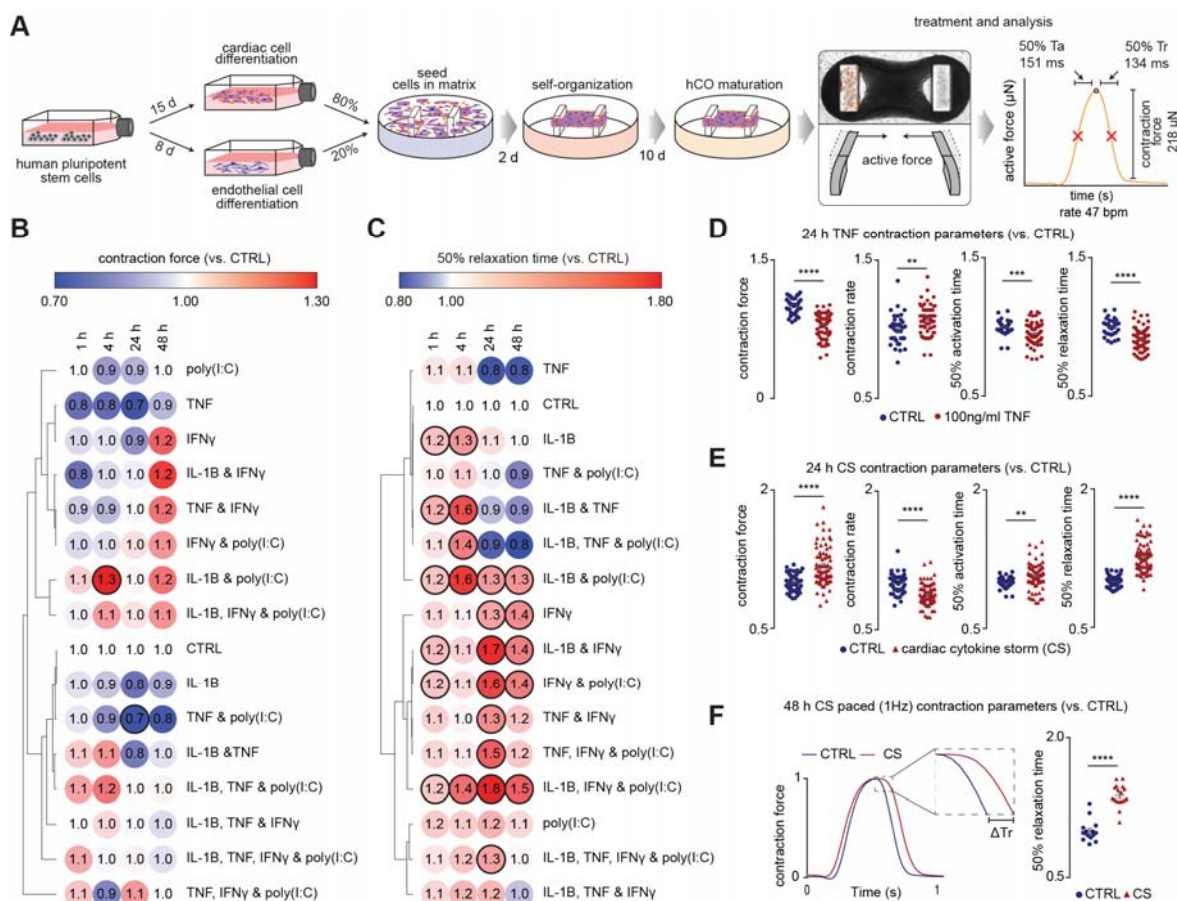
Figure 1: Identification of pro-inflammatory factors driving cardiac dysfunction.

A) Schematic of experimental pipeline. Values for overall functional parameters are the mean of n = 1100 hCO from 9 experiments used in this study.

B) Impact of inflammatory modulators on force (systolic function). Bold outline indicates p <0.05 using a one-way ANOVA with Dunnett's multiple comparisons test comparing each condition to CTRL at its' time point. n= 3-5 hCOs per condition from 1 experiment. hPSC cardiac cells- AA, Endothelial cells- RM3.5.

C) Impact of inflammatory modulators on time to 50% relaxation (diastolic function). Bold outline indicates p <0.05 using a one-way ANOVA with Dunnett's multiple comparisons test comparing each condition to CTRL at its' time point. n= 3-5 hCOs per condition from 1 experiment. hPSC cardiac cells- AA, Endothelial cells- RM3.5.

D) TNF causes systolic dysfunction. n = 37 and 63 hCOs for CTRL and TNF conditions, respectively from 6 experiments. hPSC cardiac cells- HES3, Endothelial cells- RM3.5 or CC. ** p<0.01, *** p<0.001, **** p<0.0001, using Student's t-test.

E) CS causes diastolic dysfunction n = 49 and 73 hCOs for CTRL and CS conditions, respectively from 6 experiments. hPSC cardiac cells- HES3, Endothelial cells- RM3.5 or CC. ** p<0.01, **** p<0.0001, using Student's t-test.

F) Representative force curve of hCO under control (CTRL) and CS conditions (1 Hz) 48 h after treatment. Relaxation of CTRL and CS under paced conditions (1 Hz) 48 h after treatment. n = 15 and 17 hCOs per condition, respectively, from 3 experiments. hPSC cardiac cells- HES3, Endothelial cells- RM3.5 or CC. **** p<0.0001, using Student's t-test.

Ta – time from 50% activation to peak, Tr – time from peak to 50% relaxation
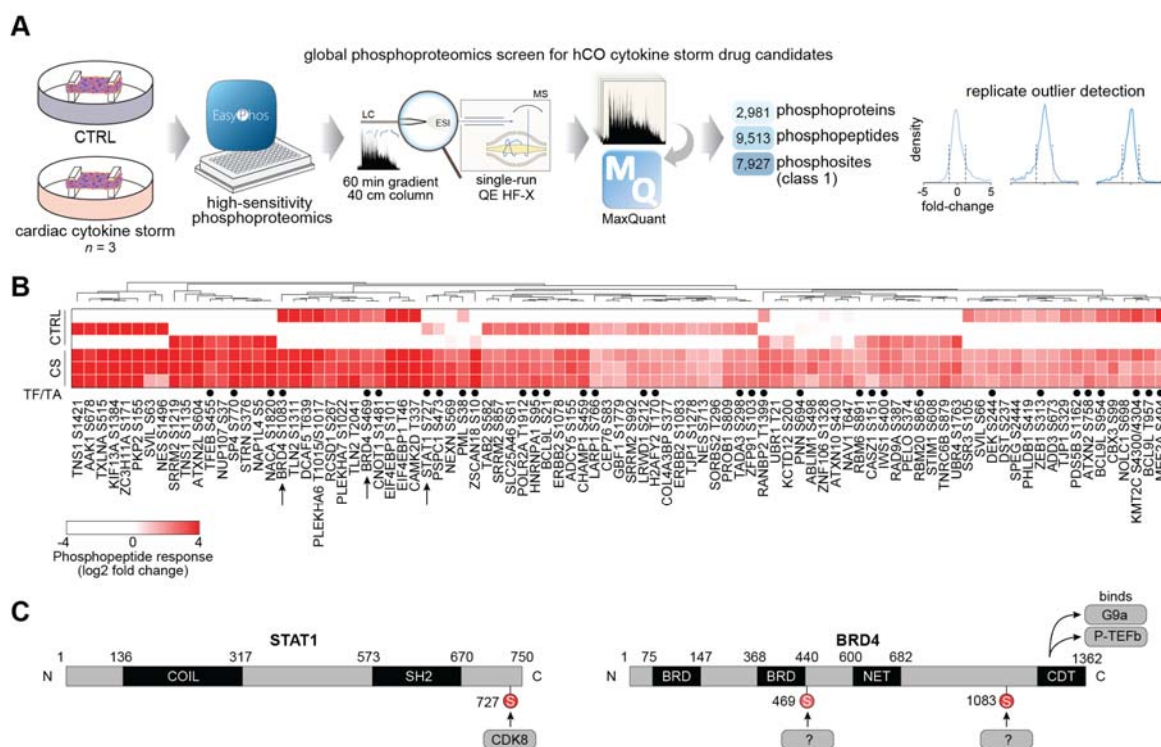
Figure 2: Phophosproteomics reveals signalling driving cardiac dysfunction.

A) Schematic of the experiment and analysis
B) Heat-map of enriched phosphopeptides in hCO following CS treatment (after 1 hour). TF/TA circles depict transcription factors and transcriptional activators.
C) Phosphorylation sites induced by CS on STAT1 and BRD4.

hPSC cardiac cells- AA, Endothelial cells- RM3.5.
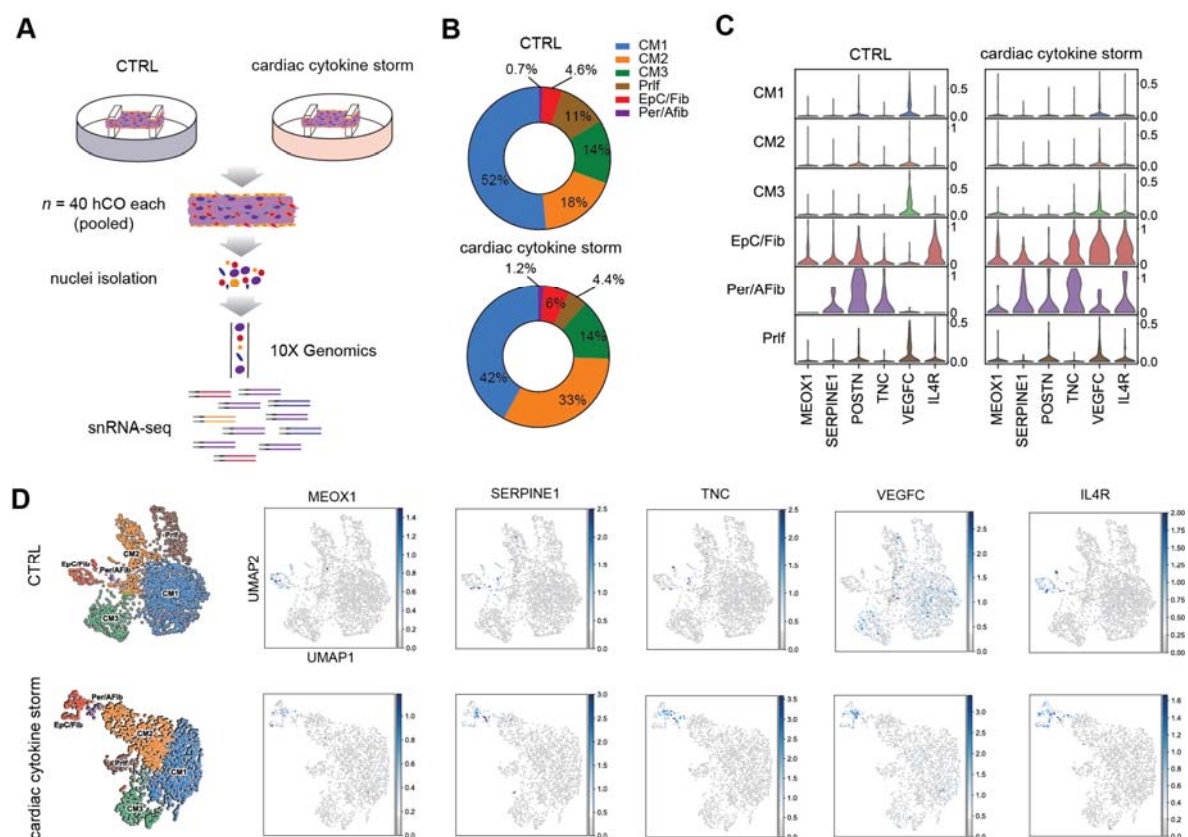
Figure 3: snRNA-seq reveals that cytokine storm activates fibroblasts in hCO

   A) Schematic of experiment
   B) Cell compositions identified in snRNA-seq
   C) Expression level of fibroblast activation markers
   D) UMAP of CTRL and cytokine storm treated hCO subpopulations and activated fibroblast markers

hPSC cardiac cells- HES3, Endothelial cells- RM3.5. CM – cardiomyocyte, Prlf – proliferating, EpC – epicardial cells, Fib – fibroblasts, Per – pericytes, Afib – activated fibroblasts.
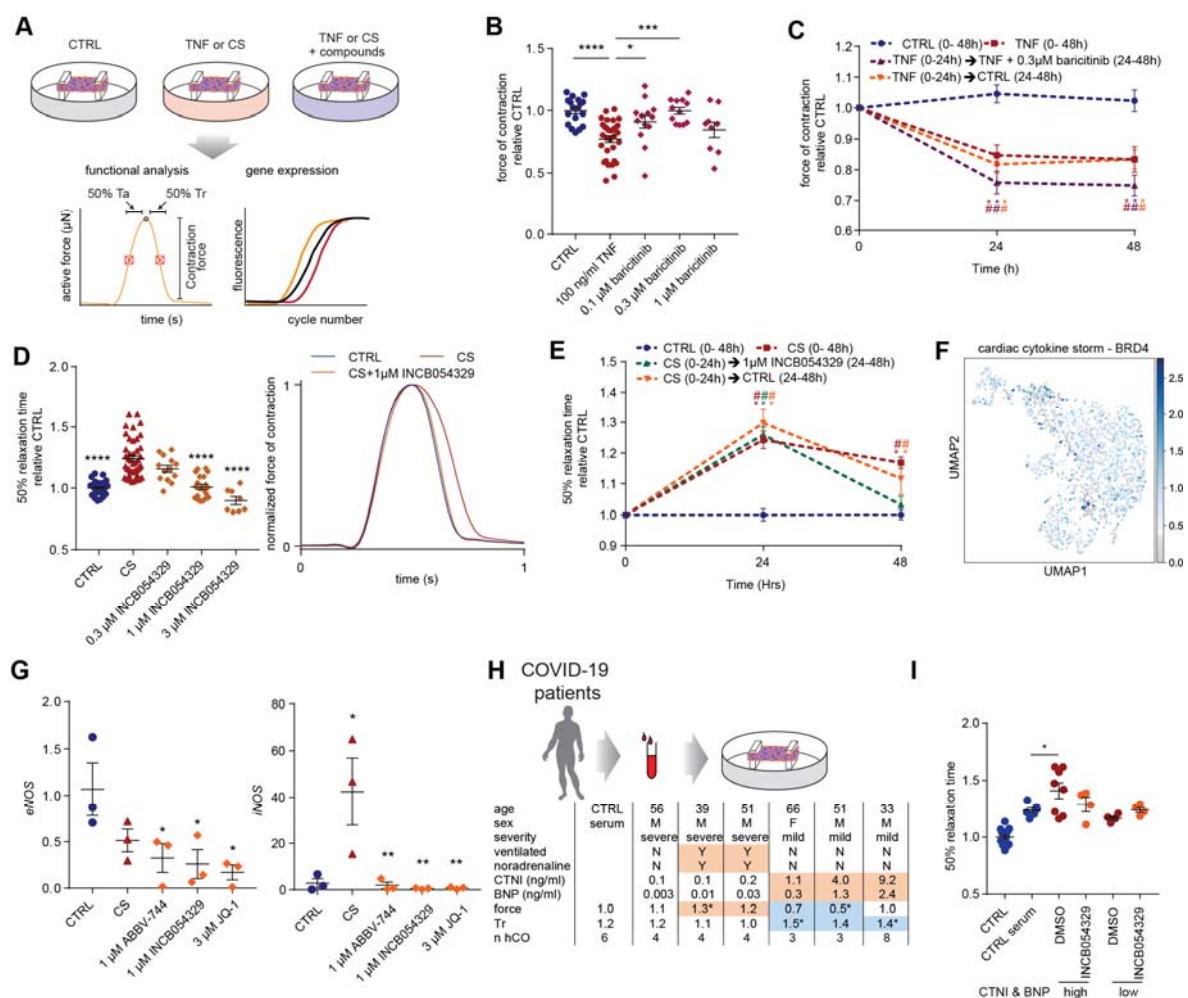
Figure 4: Drugs that improve cardiac function induced by inflammation

A) Schematic of experiment

B) Protection against systolic dysfunction (force of contraction) by baricitinib. n = 9-32 hCOs per condition from 2-3 experiments. *p<0.05, *** p<0.001, **** p<0.0001 using one-way ANOVA with Dunnett's multiple comparisons test,

C) Assessment of hCO recovery from TNF and baricitinib treatment. n = 6-12 hCOs per condition from 1-2 experiments. # p<0.05 compared to CTRL at the same time-point, and * p<0.05 compared to specific condition at 0 h with colour indicating comparison, using two-way ANOVA with Dunnett's multiple comparisons test.

D) Protection against diastolic dysfunction (time to 50% relaxation time) by INCB054329. n = 8-43 hCOs per condition from 2-4 experiments. **** p<0.0001, using one-way ANOVA with Dunnett's multiple comparisons test compared to CS.

E) Assessment of hCO recovery from CS and INCB054329 treatment. n = 6-11 hCOs per condition from 1-2 experiments. # p<0.05 compared to CTRL at the same time-point, and * p<0.05 compared to specific condition at 0 h with colour indicating comparison, using two-way ANOVA with Dunnett's multiple comparisons test.

F) BRD4 is expressed in all cell-populations in hCO

G) BRD inhibition prevents CS induced iNOS in hCO. n = 3 (2 pooled hCO) from 1 experiment. * p<0.05 and ** p<0.01, using a one-way ANOVA with Tukey's multiple comparisons test.

H) Serum from COVID-19 patients with elevated CTNI and BNP induce diastolic dysfunction. * p< 0.05 using one-way ANOVA with Dunnett's multiple comparisons test compared to CTRL serum.

I) Diastolic dysfunction induced by COVID-19 patient serum with the highest levels of CTNI and BNP is prevented by 1 µM INCB054329. n = 4-13 hCO from 1-2 experiments. * p< 0.05 using one-way ANOVA with Dunnett's multiple comparisons test compared to CTRL serum.

hPSC cardiac cells- HES3, Endothelial cells- RM3.5.
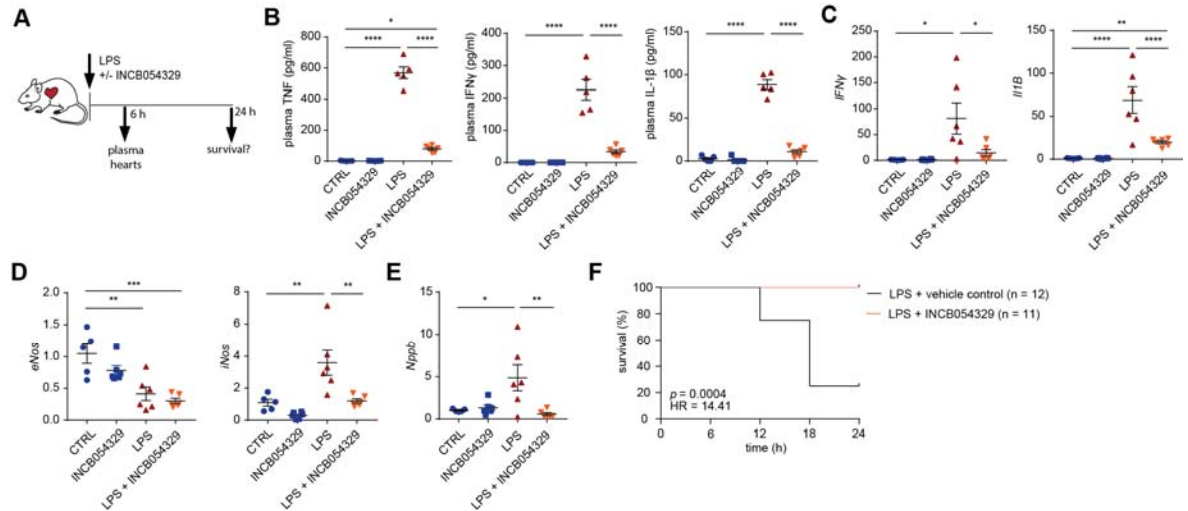
Figure 5: INCB054329 prevents inflammation, markers of cardiac pathology and death in a LPS cytokine storm mouse model

A) Schematic of experiment.
B) Cytokine levels 6 h after LPS using cytokine bead array assays. n = 5-6 mice. *p<0.05, **** p<0.0001, using one-way ANOVA with Tukey's multiple comparisons test.
C) Cytokine gene expression 6 h after LPS using qPCR. n = 5-6 mice. *p<0.05, **p<0.01, **** p<0.0001, using one-way ANOVA with Tukey's multiple comparisons test.
D) Gene expression of nitric oxides 6 h after LPS using qPCR. n = 5-6 mice. *p<0.05, **p<0.01, *** p<0.001, using one-way ANOVA with Tukey's multiple comparisons test.
E) Gene expression of Nppb (BNP) as a marker of cardiac stress 6 h after LPS using qPCR. n = 5-6 mice. *p<0.05, **p<0.01, using one-way ANOVA with Tukey's multiple comparisons test.
F) Kaplan-Meier curve of survival after LPS injection. n = 12 control and 11 INCB054329 treatment (67 mg/kg). P-value calculated using Gehan-Breslow-Wilcoxon test.
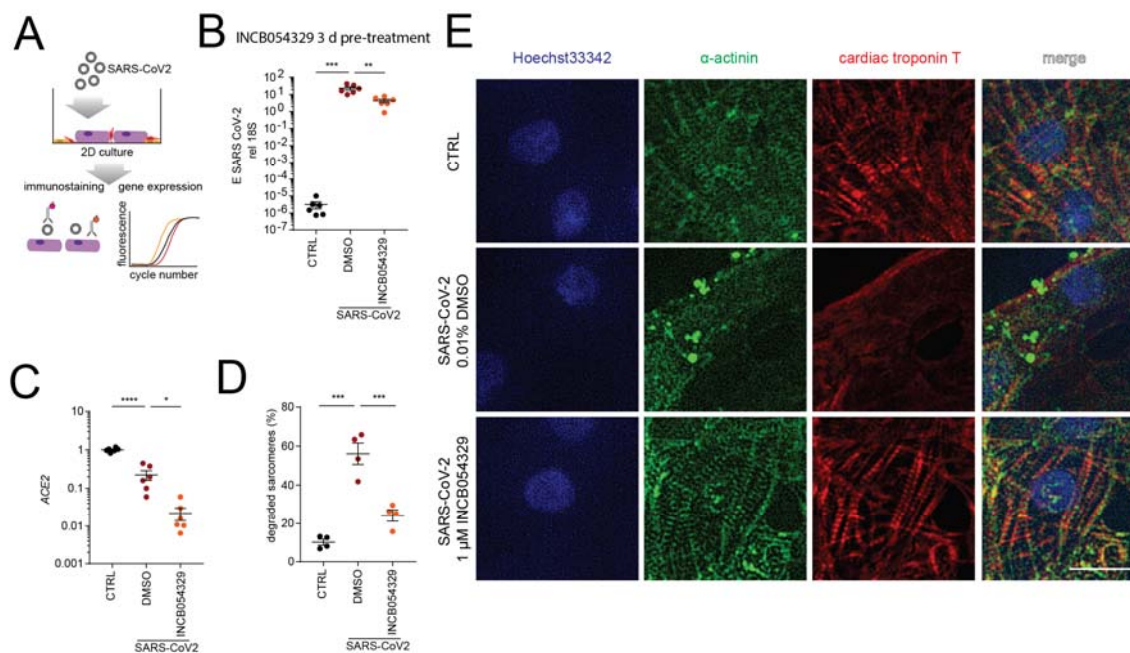
Figure 6: Pre-treatment with INCB054329 prevents SARS-CoV2 cardiac infection.

A) Schematic of the experiments.
B) E-gene expression in 2D cultured hPSC-CM 3 days after infection. Cells with pre-treated with 1 µM INCB054329 for 3 days prior to infection. n = 6 biological replicates from 2 experiments. ** p<0.01, *** p<0.001 using one-way ANOVA with Dunnett's multiple comparisons test compared to CTRL samples with no infection.
C) ACE2 expression in 2D cultured hPSC-CM 3 days after infection. Cells with pre-treated with 1 µM INCB054329 for 3 days prior to infection. n = 6 biological replicates from 2 experiments. * p<0.05, **** p<0.0001 using one-way ANOVA with Dunnett's multiple comparisons test compared to CTRL samples with no infection.
D) Quaification of cardiomyocytes with disorganized sarcomeres in 2D cultured hPSC-CM 3 days after infection. Cells with pre-treated with 1 µM INCB054329 for 3 days prior to infection. n = 4 biological replicates. *** p<0.001 using one-way ANOVA with Tukey's multiple comparisons test.
E) Representative immunostaining of cardiomyocytes. Scale bar = 20 µm.

REFERENCES

1. T. Guo *et al.*, Cardiovascular Implications of Fatal Outcomes of Patients With Coronavirus Disease 2019 (COVID-19). *JAMA Cardiology* **5**, 811-818 (2020).
2. Z. Wu, J. M. McGoogan, Characteristics of and Important Lessons From the Coronavirus Disease 2019 (COVID-19) Outbreak in China: Summary of a Report of 72 314 Cases From the Chinese Center for Disease Control and Prevention. *JAMA* **323**, 1239-1242 (2020).
3. S. Shi *et al.*, Association of Cardiac Injury With Mortality in Hospitalized Patients With COVID-19 in Wuhan, China. *JAMA Cardiology* **5**, 802-810 (2020).
4. C. Chen, H. Li, W. Hang, D. W. Wang, Cardiac injuries in coronavirus disease 2019 (COVID-19). *Journal of Molecular and Cellular Cardiology* **145**, 25-29 (2020).
5. A. Gupta *et al.*, Extrapulmonary manifestations of COVID-19. *Nature Medicine* **26**, 1017-1032 (2020).
6. P. Goyal *et al.*, Clinical Characteristics of Covid-19 in New York City. *New England Journal of Medicine* **382**, 2372-2374 (2020).
7. Y. Szekely *et al.*, The Spectrum of Cardiac Manifestations in Coronavirus Disease 2019 (COVID-19) - a Systematic Echocardiographic Study. *Circulation* **0**, (2020).
8. V. O. Puntmann *et al.*, Outcomes of Cardiovascular Magnetic Resonance Imaging in Patients Recently Recovered From Coronavirus Disease 2019 (COVID-19). *JAMA Cardiology*, (2020).
9. D. M. Del Valle *et al.*, An inflammatory cytokine signature predicts COVID-19 severity and survival. *Nature Medicine*, (2020).
10. P. S. Arunachalam *et al.*, Systems biological assessment of immunity to mild versus severe COVID-19 infection in humans. *Science* **369**, 1210-1220 (2020).
11. A. M. Feldman *et al.*, The role of tumor necrosis factor in the pathophysiology of heart failure. *Journal of the American College of Cardiology* **35**, 537-544 (2000).
12. P. Horby *et al.*, Effect of Dexamethasone in Hospitalized Patients with COVID-19: Preliminary Report. *medRxiv*, 2020.2006.2022.20137273 (2020).
13. N. Mangalmurti, C. A. Hunter, Cytokine Storms: Understanding COVID-19. *Immunity* **53**, 19-25 (2020).
14. R. J. Mills *et al.*, Drug Screening in Human PSC-Cardiac Organoids Identifies Pro-proliferative Compounds Acting via the Mevalonate Pathway. *Cell stem cell* **24**, 895-907.e896 (2019).
15. R. J. Mills *et al.*, Functional screening in human cardiac organoids reveals a metabolic mechanism for cardiomyocyte cell cycle arrest. *Proceedings of the National Academy of Sciences* **114**, E8372-E8381 (2017).
16. C. Huang *et al.*, Clinical features of patients infected with 2019 novel coronavirus in Wuhan, China. *The Lancet* **395**, 497-506 (2020).
17. H. K. Voges *et al.*, Development of a human cardiac organoid injury model reveals innate regenerative potential. *Development (Cambridge, England)* **144**, 1118-1127 (2017).
18. G. A. Quaife-Ryan *et al.*, Multicellular Transcriptional Analysis of Mammalian Heart Regeneration. *Circulation* **136**, 1123-1139 (2017).
19. N. R. Tucker *et al.*, Transcriptional and Cellular Diversity of the Human Heart. *Circulation* **0**, (2020).
20. R. Gilsbach *et al.*, Distinct epigenetic programs regulate cardiac myocyte development and disease in the human heart in vivo. *Nature communications* **9**, 391 (2018).
21. N. T. Vasudevan *et al.*, Gβγ-independent recruitment of G-protein coupled receptor kinase 2 drives tumor necrosis factor α-induced cardiac β-adrenergic receptor dysfunction. *Circulation* **128**, 377-387 (2013).
22. T. Kubota *et al.*, Dilated Cardiomyopathy in Transgenic Mice With Cardiac-Specific Overexpression of Tumor Necrosis Factor-&#x3b1. *Circulation research* **81**, 627-635 (1997).
23. S. P. Levick, P. H. Goldspink, Could interferon-gamma be a therapeutic target for treating heart failure? *Heart failure reviews* **19**, 227-236 (2014).

24.   E. J. Needham, B. L. Parker, T. Burykin, D. E. James, S. J. Humphrey, Illuminating the dark phosphoproteome. *Science Signaling* **12**, eaau8645 (2019).

25.   S. J. Humphrey, S. B. Azimifar, M. Mann, High-throughput phosphoproteomics reveals in vivo insulin signaling dynamics. *Nature biotechnology* **33**, 990-995 (2015).

26.   S. J. Humphrey, O. Karayel, D. E. James, M. Mann, High-throughput and high-sensitivity phosphoproteomics with the EasyPhos platform. *Nature Protocols* **13**, 1897-1916 (2018).

27.   M. Alexanian *et al.*, A Transcriptional Switch Governing Fibroblast Plasticity Underlies Reversibility of Chronic Heart Disease. *bioRxiv*, 2020.2007.2021.214874 (2020).

28.   V. S. Hahn *et al.*, Endomyocardial Biopsy Characterization of Heart Failure With Preserved Ejection Fraction and Prevalence of Cardiac Amyloidosis. *JACC: Heart Failure*, (2020).

29.   S. M. Schumacher *et al.*, Paroxetine-mediated GRK2 inhibition reverses cardiac dysfunction and remodeling after myocardial infarction. *Science translational medicine* **7**, 277ra231-277ra231 (2015).

30.   S. Guo, R. L. Carter, L. A. Grisanti, W. J. Koch, D. G. Tilley, Impact of paroxetine on proximal β-adrenergic receptor signaling. *Cell Signal* **38**, 127-133 (2017).

31.   T. Evron, T. L. Daigle, M. G. Caron, GRK2: multiple roles beyond G protein-coupled receptor desensitization. *Trends Pharmacol Sci* **33**, 154-164 (2012).

32.   P. Richardson *et al.*, Baricitinib as potential treatment for 2019-nCoV acute respiratory disease. *Lancet* **395**, e30-e31 (2020).

33.   I. Sadzak *et al.*, Recruitment of Stat1 to chromatin is required for interferon-induced serine phosphorylation of Stat1 transactivation domain. *Proceedings of the National Academy of Sciences of the United States of America* **105**, 8944-8949 (2008).

34.   J. Bancerek *et al.*, CDK8 kinase phosphorylates transcription factor STAT1 to selectively regulate the interferon response. *Immunity* **38**, 250-262 (2013).

35.   T. Rzymski *et al.*, SEL120-34A is a novel CDK8 inhibitor active in AML cells with high levels of serine phosphorylation of STAT1 and STAT5 transactivation domains. *Oncotarget* **8**, 33779-33795 (2017).

36.   M. H. Hofmann *et al.*, Selective and Potent CDK8/19 Inhibitors Enhance NK-Cell Activity and Promote Tumor Surveillance. *Molecular Cancer Therapeutics* **19**, 1018-1030 (2020).

37.   M. C. Stubbs *et al.*, The Novel Bromodomain and Extraterminal Domain Inhibitor INCB054329 Induces Vulnerabilities in Myeloma Cells That Inform Rational Combination Strategies. *Clinical Cancer Research* **25**, 300-311 (2019).

38.   P. Filippakopoulos *et al.*, Selective inhibition of BET bromodomains. *Nature* **468**, 1067-1073 (2010).

39.   E. J. Faivre *et al.*, Selective inhibition of the BD2 bromodomain of BET proteins in prostate cancer. *Nature* **578**, 306-310 (2020).

40.   T. Gagliano-Jucá *et al.*, Androgen Deprivation Therapy Is Associated With Prolongation of QTc Interval in Men With Prostate Cancer. *J Endocr Soc* **2**, 485-496 (2018).

41.   L. Huang *et al.*, Cardiac Involvement in Patients Recovered From COVID-2019 Identified Using Magnetic Resonance Imaging. *JACC: Cardiovascular Imaging*, 3427 (2020).

42.   M. S. Stratton *et al.*, Dynamic Chromatin Targeting of BRD4 Stimulates Cardiac Fibroblast Activation. *Circulation research* **125**, 662-677 (2019).

43.   M. S. Stratton, S. M. Haldar, T. A. McKinsey, BRD4 inhibition for the treatment of pathological organ fibrosis. *F1000Res* **6**, F1000 Faculty Rev-1015 (2017).

44.   W. J. Paulus, C. Tschöpe, A Novel Paradigm for Heart Failure With Preserved Ejection Fraction: Comorbidities Drive Myocardial Dysfunction and Remodeling Through Coronary Microvascular Endothelial Inflammation. *Journal of the American College of Cardiology* **62**, 263-271 (2013).

45.   M. Finkel *et al.*, Negative inotropic effects of cytokines on the heart mediated by nitric oxide. *Science* **257**, 387-389 (1992).

46.   G. G. Schiattarella *et al.*, Nitrosative stress drives heart failure with preserved ejection fraction. *Nature* **568**, 351-356 (2019).

47.   A. Sharma *et al.*, Human iPSC-Derived Cardiomyocytes Are Susceptible to SARS-CoV-2 Infection. *Cell Rep Med* **1**, 100052-100052 (2020).

48.   D. Lindner *et al.*, Association of Cardiac Infection With SARS-CoV-2 in Confirmed COVID-19 Autopsy Cases. *JAMA Cardiology*, (2020).

49.   K. E. Runte *et al.*, Relaxation and the Role of Calcium in Isolated Contracting Myocardium From Patients With Hypertensive Heart Disease and Heart Failure With Preserved Ejection Fraction. *Circ Heart Fail* **10**, (2017).

50.   M. Nishiga, D. W. Wang, Y. Han, D. B. Lewis, J. C. Wu, COVID-19 and cardiovascular disease: from basic mechanisms to clinical perspectives. *Nature Reviews Cardiology*, (2020).

51.   E. Nicodeme *et al.*, Suppression of inflammation by a synthetic histone mimic. *Nature* **468**, 1119-1123 (2010).

52.   Q. Duan *et al.*, BET bromodomain inhibition suppresses innate inflammatory and profibrotic transcriptional networks in heart failure. *Science translational medicine* **9**, eaah5084 (2017).

53.   A. G. Cochran, A. R. Conery, R. J. Sims, Bromodomains: a new target class for drug development. *Nature Reviews Drug Discovery* **18**, 609-628 (2019).

ACKNOWLEDGEMENTS

DECLARATION OF INTERESTS

R.J.M., J.E.H., G.A.Q.-R., D.M.T. and E.R.P. are listed as co-inventors on pending patents held by The University of Queensland and QIMR Berghofer Medical Research Institute that relate to cardiac organoid maturation and putative cardiac regeneration therapeutics. J.E.H. is a co-inventor on licensed patents held by the University of Goettingen. R.J.M, E.R.P., D.M.T., B.G. and J.E.H. are co-founders, scientific advisors and stockholders in Dynomics Inc. D.M.T. and B.G. are employees of Dynomics Inc. /Dynomics Pty Ltd. QIMR Berghofer Medical Research Institute has filed a patent on the use of BRD inhibitors.

AUTHOR CONTRIBUTIONS

R.J.M., S.J.H., G.A.Q-R., S.K., M.L., L.T.R., R.R., D.J.R., T.L., W.Z., L.L., C.M-K., D.A-B., K.K., T.B., J.E.H., performed experiments, L.D., H.K.V.,L.T.R., E.M., developed cardiac organoid cultures, R.J.M., S.J.H., P.R.J.F., Q.A.Q-R., M.L., N.R.M., B.G., D.T., R.R., K.S., E.R.P., T.B., J.E.H., analysed data, J.M., provided clinical samples, R.J.M., S.J.H., M.J.S., C.R.E., K.P.A.MD., T.B., D.A.E, K.S., A.S., D.E.J, J.E.H, designed the project, R.J.M., S.J.H., M.J.S., C.R.E., K.P.A.MD., R.R., K.S., E.R.P., A.S., T.B., D.E.J, J.E.H, interpreted data, R.J.M., S.J.H., D.E.J, J.E.H wrote the manuscript, all authors edited the manuscript.